

Supporting Information

A computational study on the photophysics of methylpheophorbide a

Hernán Rueda Bueno^a, Julio R. Pinzón^b, Martha C. Daza^a, Markus Doerr^a*

*^aGrupo de Bioquímica Teórica, Universidad Industrial de Santander, Carrera 27, Calle 9,
Bucaramanga, Colombia*

*^bLaboratorio de Síntesis Orgánica, Universidad Industrial de Santander, Carrera 27, Calle 9,
Bucaramanga, Colombia*

* Corresponding author

Table of Contents

1. Excited state properties.....	2
1.1 Excited state dipole moments.....	2
1.2 Difference densities.....	2
1.3 Geometries of the ground and excited state minima.....	2
2. Choice of the computational parameters.....	4
2.1 Effect of the density functional and the Tamm-Dancoff approximation on the VEEs.....	4
2.2 Effect of the basis set and the Tamm-Dancoff approximation on the VEEs.....	4
2.3 Effect of the functional and basis sets on the calculated Q band in toluene.....	5
2.4 Effect of the number of points of the correlation function on the absorption and fluorescence spectrum.....	6
2.5 Effect of discarding vibrational modes on the absorption and fluorescence spectra.....	7
3. Absorption and fluorescence processes.....	10
3.1 Effect of the level of theory on the adiabatic energy differences of the low-lying singlet states..	10
3.2 Effect of the level of theory on the fluorescence rate constants.....	11
3.3 Effect of different parameters on the calculated fluorescence spectra.....	11
4. Intersystem crossing.....	12
4.1 Adiabatic energy difference between the lowest singlet excited state and the low-lying triplet states.....	12
4.2 Effect of discarding vibrational modes on the ISC rate constants.....	12
4.3 Derivatives of the SOCMEs with respect to the corresponding vibrational modes.....	13
4.4 Effect of the Gaussian linewidth on the ISC rate constants.....	21
4.5 Effect of the level of theory, FC and FCHT approximations on the k_{ISC}	22
4.6 The five largest coupling vibrational normal modes.....	22

1. Excited state properties

1.1 Excited state dipole moments

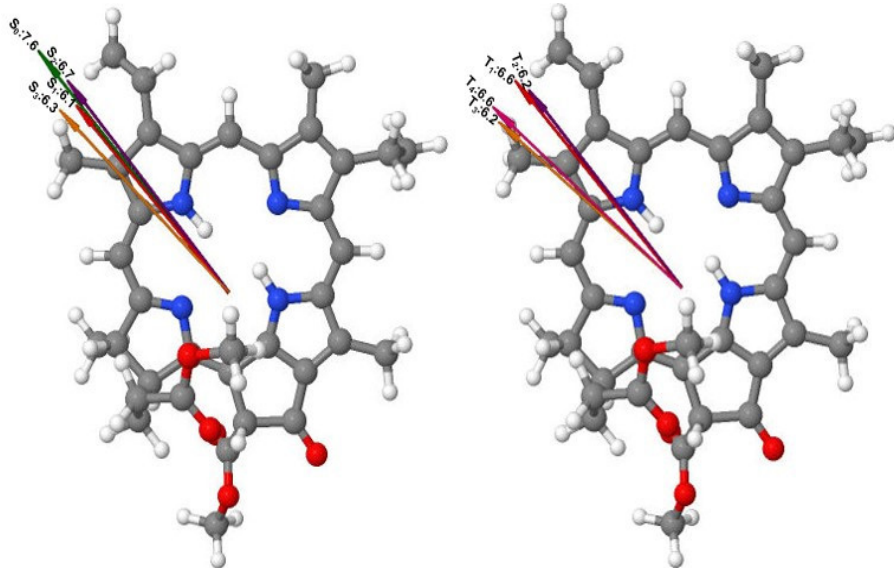


Fig. S1. Negative dipole moments of the lowest singlet S_0 - S_3 and triplet T_1 - T_4 excited states in MPH, calculated at the CAM-B3LYP/def2-SVP excited state geometries. The magnitudes of the dipole moments are given in Debye.

1.2 Difference densities

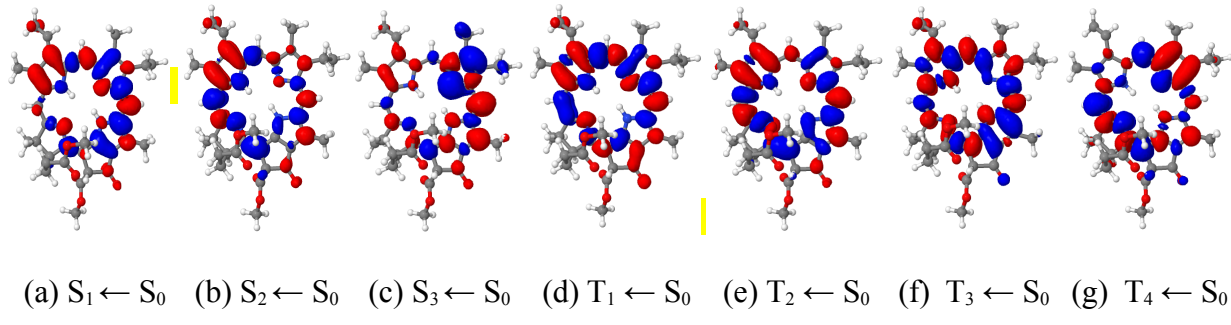


Fig. S2. Difference densities (cutoff 0.0005) of the excited states at the S_0 geometry in toluene. Regions with decreased electron density compared to the electronic ground state are shown in red, regions with increased electron density are shown in blue.

1.3 Geometries of the ground and excited state minima

The optimized structures of S_0 - S_2 and T_1 - T_3 are shown in Fig. S3. The optimization of the T_2 excited state was a challenging task. TDA-DFT geometry optimizations of the T_2 state starting at the S_0 , and S_1 minima were unsuccessful. However, a TD-DFT geometry optimization of the T_2 state from the S_0 without the Tamm-Dancoff approximation succeeded in finding a minimum of the T_2 state.

Due to the rigid structure of the molecule, the geometric differences between the excited state geometries are small. The main differences include the C-C methine bridge distances, the C-C

distances of the first pyrrole ring and the C–N distances of the deprotonated pyrrole rings, which are also characteristic of porphyrin.

In the S_1 state, the elongation of the C₂–C₃, C₆–C₇, C₆–N₂₂, C₉–C₁₀, C₁₁–C₁₂ and C₁₅–C₁₆ distances amounts to 2 pm. While the C₄–C₅ distance is elongated by 3 pm, the C₅–C₆ distance is shortened by the same value. Moreover, the C₁₉–C₂₀–C₁ methine bridge exhibits an asymmetric stretching pattern. In the S_2 state, the C₃–C₄, C₅–C₆, C₁₉–C₂₀ and C₁₆–N₂₄ distances are shortened by 2 pm; the C₂–C₃, C₄–C₅ and C₁₉–N₂₄ distances are elongated by 3 pm. The main difference of this state is the elongation of the C₁–C₂₀ distance which amounts to 4 pm. In the S_3 state, the most significant structural changes are elongations of the C₉–C₁₀, C₁₁–C₁₂, C₂–C₃, C₄–C₅, C₆–N₂₂, C₁₅–C₁₆, C₁₉–C₂₄, C₂₀–C₁ distances by 3, 3, 2, 2, 2, 2, 2 pm and shortening of the C₉–N₂₂, C₁₀–C₁₁ and C₁₆–N₂₄ by 2 pm. In the T_1 state, the C₄–C₅ distance and the C₅–C₆ distance are extended by 6 pm and shortened by 5 pm, respectively. The C₃–C₄, C₉–N₂₂ distances are shortened by 4 pm and the C₆–N₂₂ distance is elongated by 4 pm. The T_2 state is mainly characterized by the shortening of the C₅–C₆, C₁₆–N₂₄ and C₁₉–C₂₀ distances, which amount to 4, 3 and 3 pm, and the elongation of the C₄–C₅, C₁₉–N₂₄, C₁₅–C₁₆, C₂₀–C₁, C₆–C₇ and C₈–C₉ distances by 5, 4, 3, 3, 3 and 3 pm. In the T_3 state, the principal variations are the C₉–C₁₀, C₁₁–C₁₂ distance elongation of 4 pm and the C₁₀–C₁₁ distance shortening of 3 pm.

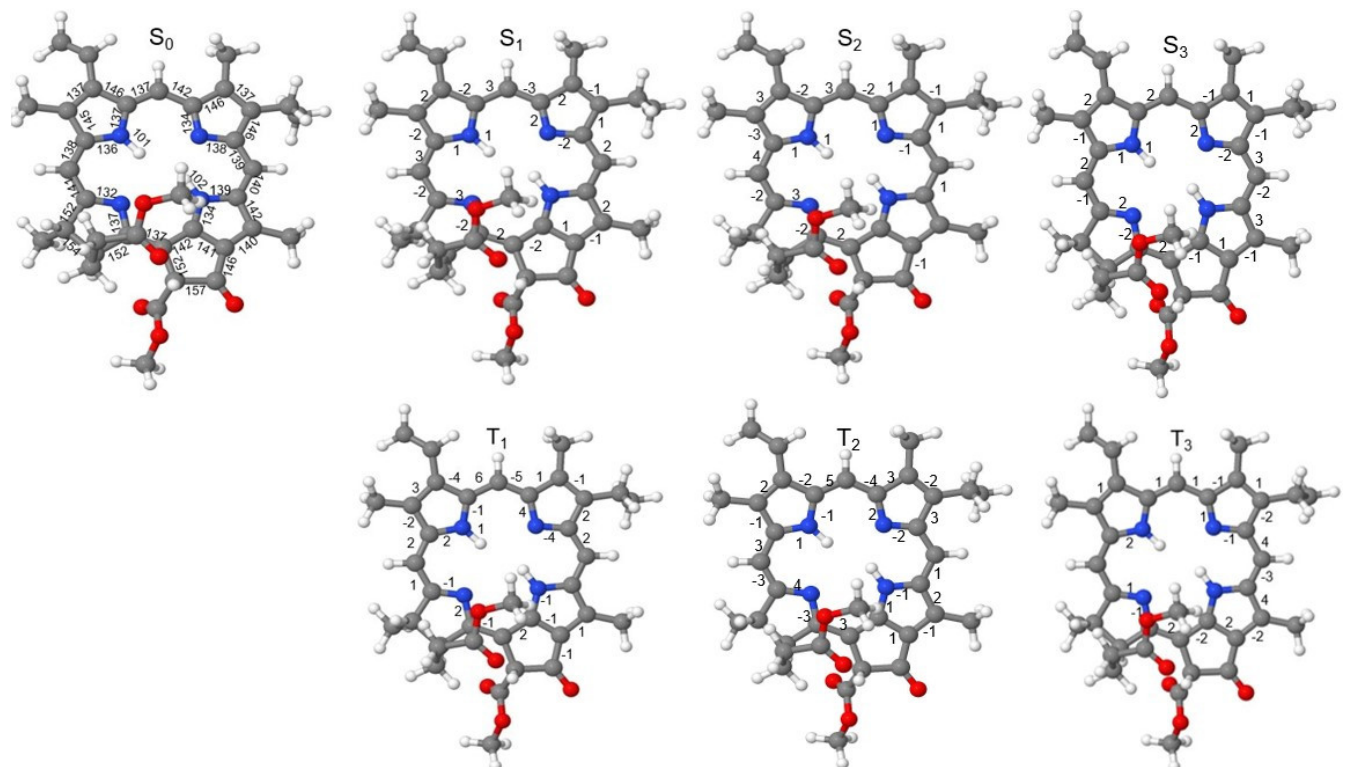


Fig. S3. Selected bond lengths (in pm) of the ground state, and differences relative to the ground state structure. Only non-zero values are given.

2. Choice of the computational parameters

2.1 Effect of the density functional and the Tamm-Danoff approximation on the VEEs

In order to test the effect of the Tamm-Danoff approximation on the calculated VEE, we calculated the VEEs with and without TDA (Fig. S4). The effect of the TDA is a blue-shift of up to 0.16 eV with respect to the calculated TD-DFT energies, resulting in deviations of the calculated VEE of up to 0.49 eV from the experimental band maxima. Similar blue shifts have been observed using this functional in a recent study of the absorption spectra of phthalocyanins.¹

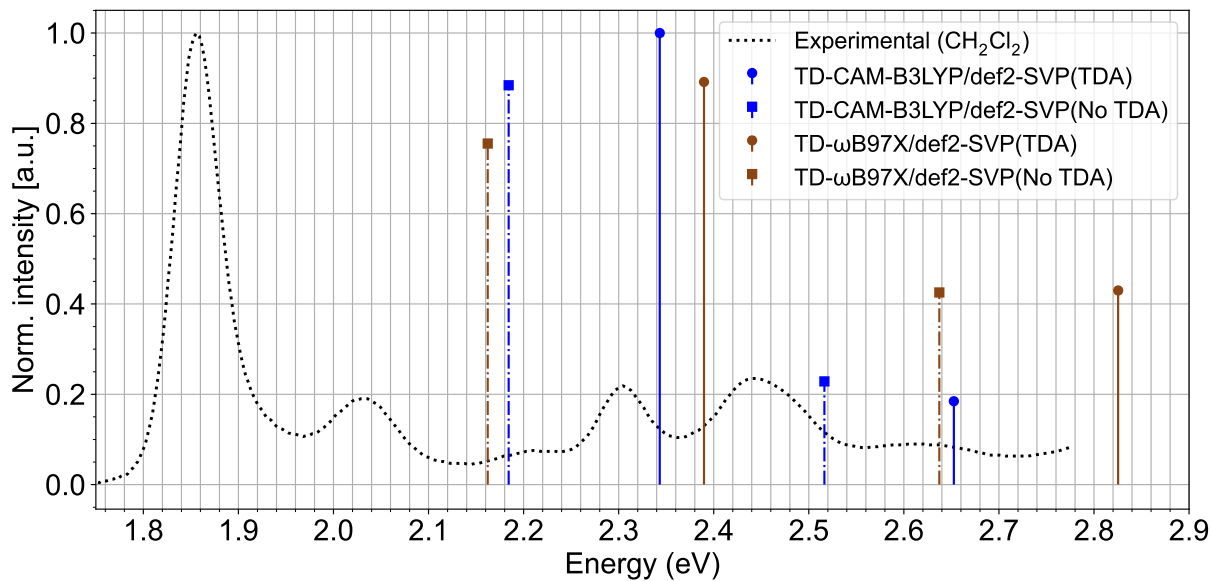


Fig. S4. Effect of the density functional and the TDA approximation on the vertical excitation energies (eV) associated with the first (S_1) and second (S_2) singlet excited states computed at the ground state geometry.

2.2 Effect of the basis set and the Tamm-Danoff approximation on the VEEs

The effect of the basis set on the calculated absorption spectrum of MPh was also investigated (Fig. S5). The effect of the smaller def2-SVP basis set under TDA or full TD-DFT on the absorption spectrum is blue shift of the excitation energies of ≈ 0.04 eV. Since the effect of the basis set is small and the basis set def2-TZVP is computationally more expensive (particularly for the numerical computation of the vibrational frequencies of the excited states) than the def2-SVP basis set, the latter was chosen. The CAM-B3LYP/def2-SVP VEE is about 0.5 eV higher than the experimental band maximum, for the S_2 transition the difference is about 0.3 eV. It should be noted that the band maximum and the vertical excitation energy do not coincide and that the VEE is more than 0.1 eV higher than the calculated band maximum.²

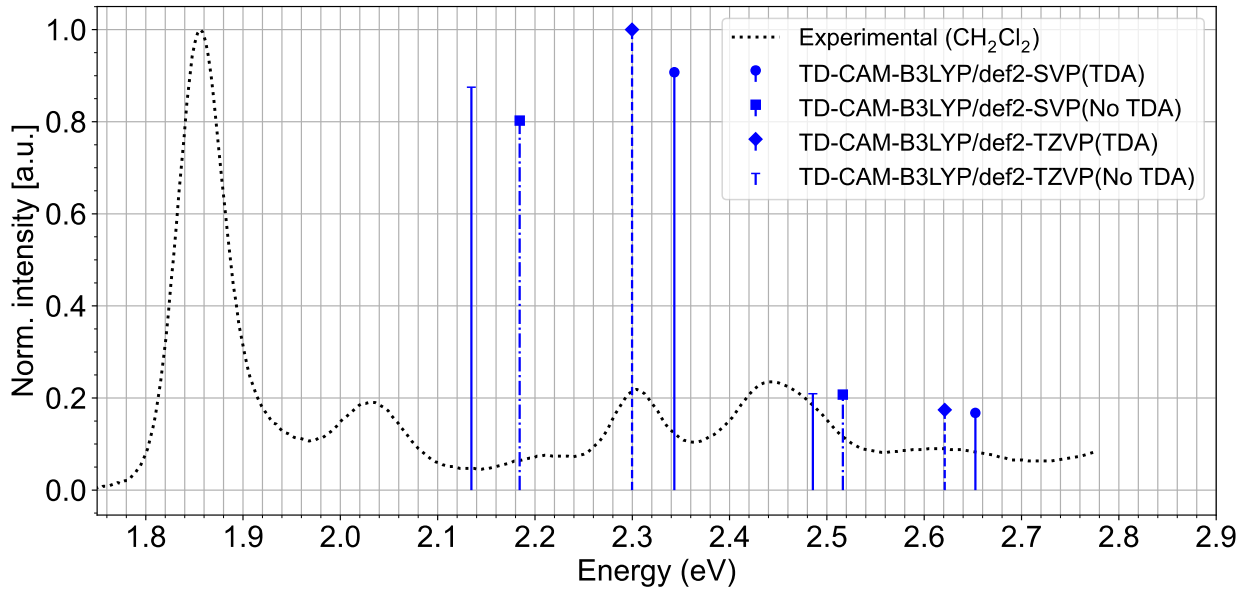


Fig. S5. Effect of the basis set and the TDA approximation on the vertical excitation energies (eV) associated with the first (S_1) and second (S_2) singlet excited states computed at the ground state geometry. All calculations were performed using the CAM-B3LYP/def2-SVP optimized structure.

2.3 Effect of the functional and basis sets on the calculated Q band in toluene

To investigate the effect of the level of theory on the absorption properties of MPh, we used the CAM-B3LYP/def2-SVP optimized geometries and performed single point calculations with the density functionals CAM-B3LYP, ω B97X, PBE0 and the basis sets def2-SVP, def2-TZVP (see Table S1). The calculated VEEs for S_1 are found to be very similar with the three functionals, with differences of ≤ 0.1 eV. Larger differences between the three functionals are observed for the S_2 state. The utilization of the smaller, less computationally demanding def2-SVP basis has a minimal impact on the VEEs, with blue shifts of less than 0.05 eV observed for the S_1 and S_2 transitions with the CAM-B3LYP functional.

Table S1. TD-DFT spectroscopic parameters for the Q band calculated in toluene with different density functionals and bases and using the CAM-B3LYP/def2-SVP optimized structure.

Transition	Exp. (eV) ^a	Functional	def2-SVP			def2-TZVP		
			VEE (eV)	λ (nm)	$f_{\text{osc.}}$	VEE (eV)	λ (nm)	$f_{\text{osc.}}$
$S_0 \rightarrow S_1$	1.85	CAM-B3LYP	2.343	529.1	0.3302	2.300	539.1	0.3639
		ω B97X	2.390	518.8	0.2945	2.346	528.4	0.3190
		PBE0	2.290	541.4	0.3258	2.251	550.7	0.3613
$S_0 \rightarrow S_2$	2.31	CAM-B3LYP	2.653	467.4	0.0610	2.621	473.0	0.0634
		ω B97X	2.826	438.8	0.1420	2.801	442.6	0.1574
		PBE0	2.511	493.8	0.0427	2.479	500.2	0.0399

^aRef.³ maximum of the absorption band in toluene.

2.4 Effect of the number of points of the correlation function on the absorption and fluorescence spectrum

When all vibrational modes are included in the calculation of the absorption and fluorescence spectrum, the bands have an unrealistic shape (see Figs. S6 and S7). In order to test whether a larger number of grid points of the correlation function results in more realistic spectra, we performed the calculations with higher number of grid points. As can be seen, increasing the number of points in the correlation function for absorption and fluorescence did not result in better spectra.

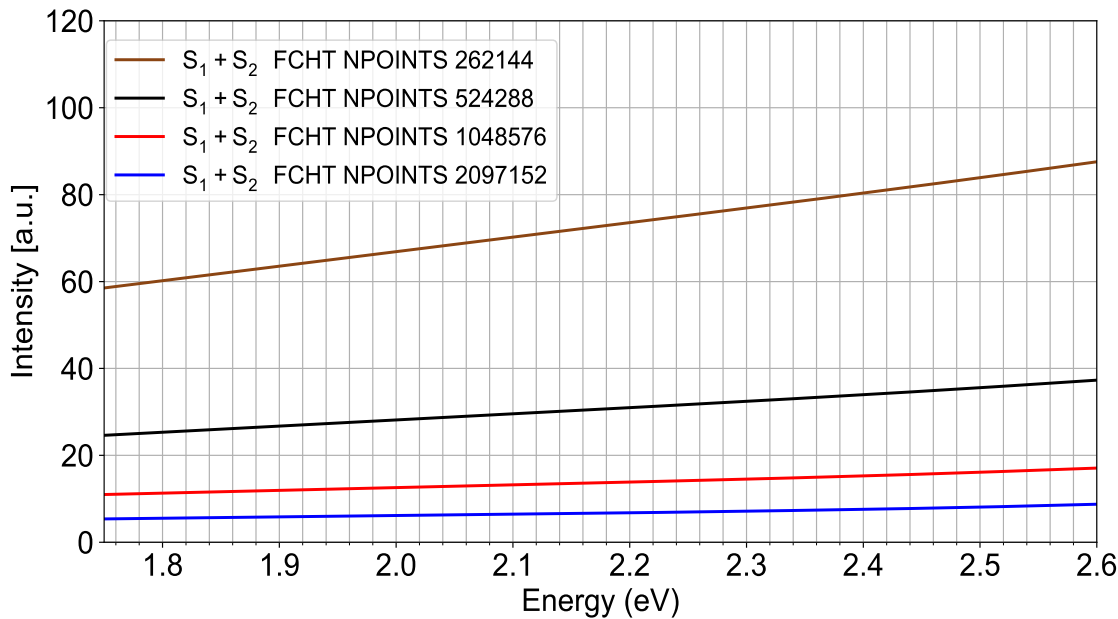


Fig. S6. Effect of the number of grid points used in the integration of the correlation function on the Q-band region of the absorption spectrum employing the adiabatic Hessian model, and including Franck-Condon and Herzberg-Teller (FCHT) terms at 298.15K. The Gaussian bandwidth was set to 150 cm⁻¹ and all vibrational modes were included.

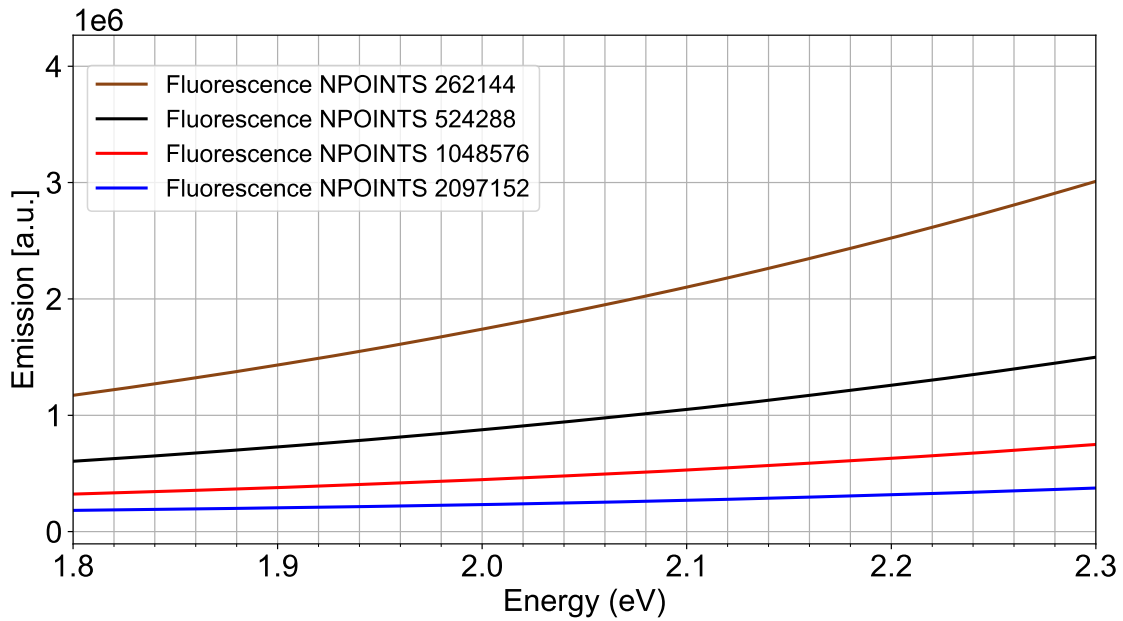


Fig. S7. Effect of the number of grid points used in the integration of the correlation function on the fluorescence spectrum employing the adiabatic Hessian model, and including Franck-Condon and Herzberg-Teller (FCHT) terms at 298.15K. The Gaussian bandwidth was set to 150 cm^{-1} and all vibrational modes were included.

2.5 Effect of discarding vibrational modes on the absorption and fluorescence spectra

The effect of discarding vibrational modes on the absorption and fluorescence spectra is shown in Figs. S8 and S9. Increasing the threshold for discarding vibrational modes to more than 300 cm^{-1} has only small effects on the band shape and the fluorescence rate (Fig. S10). Discarding only vibrational modes below 100 cm^{-1} results in unrealistic spectra.

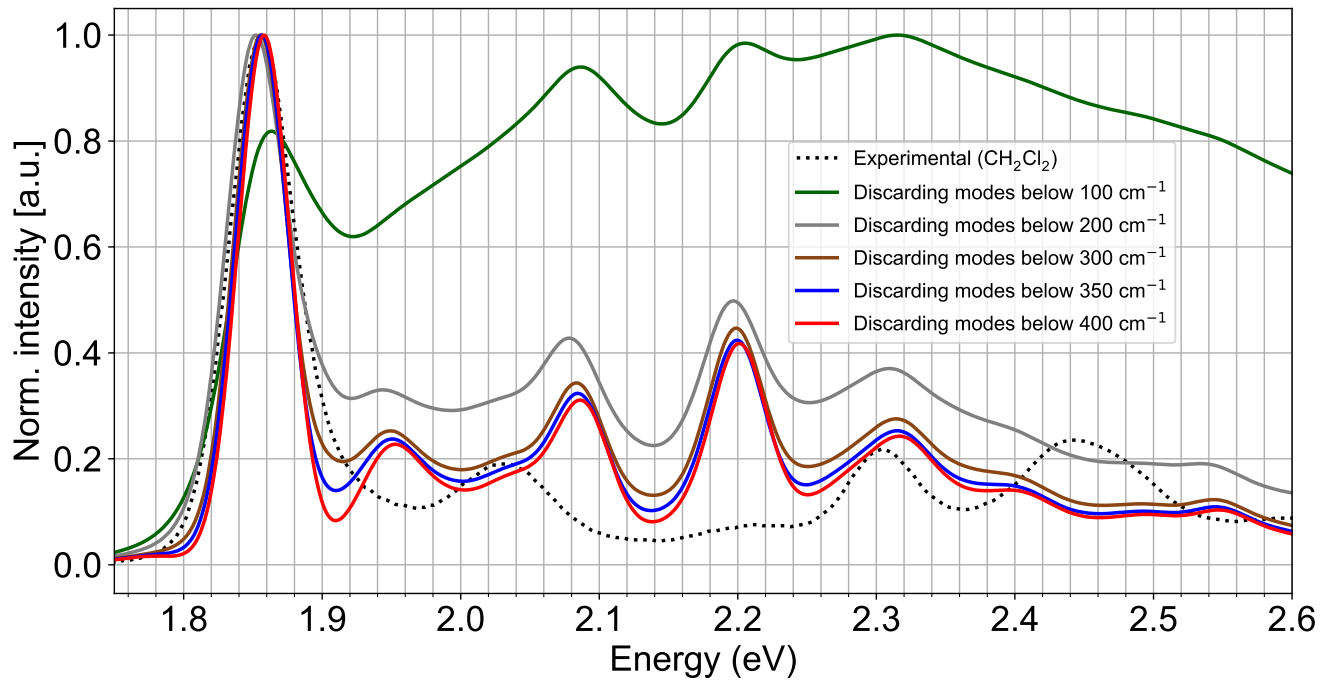


Fig. S8. Effect of discarding vibrational modes on the absorption spectrum, employing the adiabatic Hessian model, and including Franck-Condon and Herzberg-Teller (FCHT) terms at 298.15 K. The Gaussian bandwidth was set to 150 cm^{-1} . The default value of 262144 was used for the number of points of the correlation functions. All calculated spectra were shifted by 0.32 eV to align with the experimental band maximum.

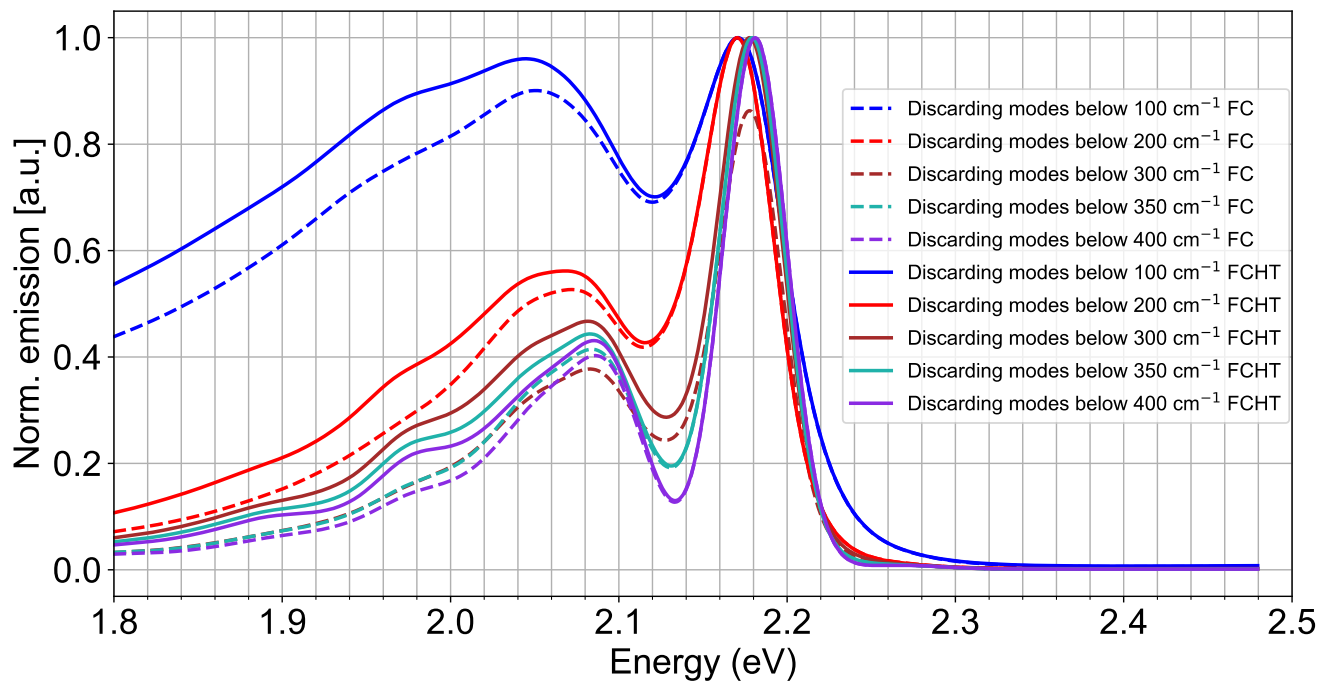


Fig. S9. Effect of discarding vibrational modes on the fluorescence spectrum, employing the adiabatic Hessian model, and including Franck-Condon (FC) and Franck-Condon and Herzberg-Teller (FCHT) terms at 298.15 K. The Gaussian bandwidth was set to 150 cm^{-1} . The default value of 262144 was used for the number of points of the correlation functions.

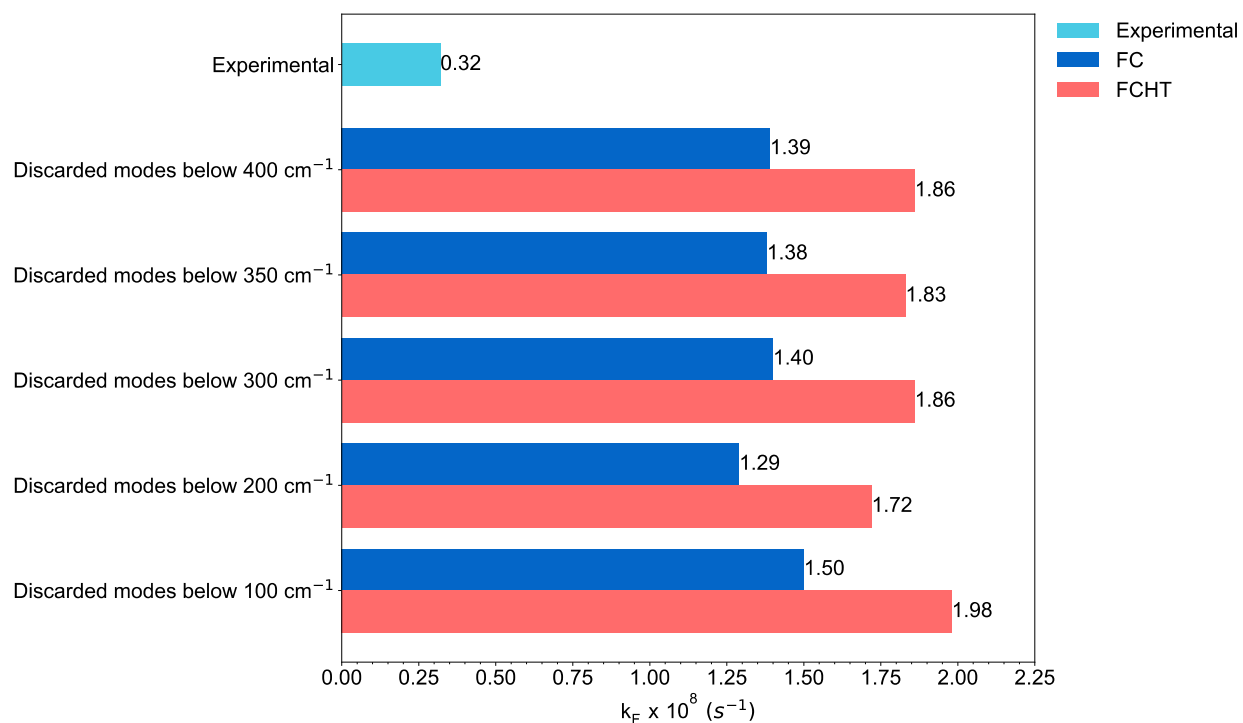


Fig. S10. Fluorescence rate constants obtained with different frequency thresholds for discarding vibrational modes, including Franck-Condon (FC) and Franck-Condon and Herzberg-Teller (FCHT) terms. The CAM-B3LYP/def2-SVP optimized geometry was used in all calculations.

3. Absorption and fluorescence processes

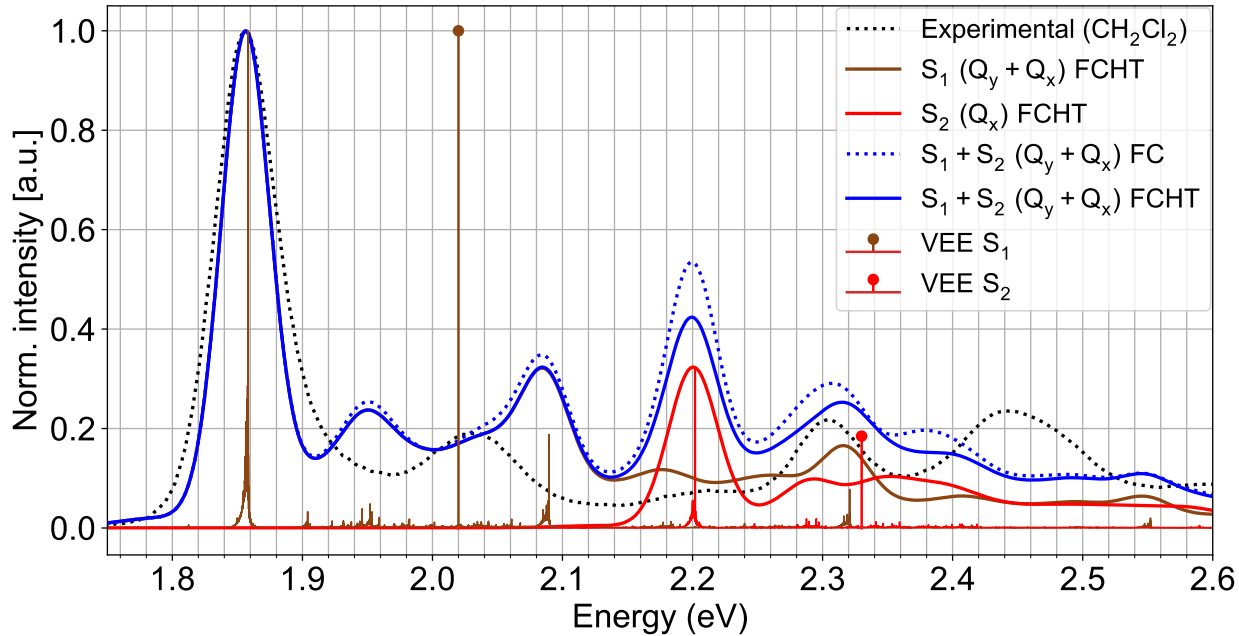


Fig. S11. Computed vibronic structure and stick spectrum of the Q-band employing the adiabatic Hessian approximation, Franck-Condon and Franck-Condon-Herzberg-Teller contributions at 298.15K. The Gaussian linewidth was set to 150 cm^{-1} and vibrational modes below 350 cm^{-1} were removed. The calculated spectra and VEEs were shifted by 0.32 eV to align with the experimental band maximum.

3.1 Effect of the level of theory on the adiabatic energy differences of the low-lying singlet states

Table S2. Adiabatic energy differences between the lowest singlet excited state and the ground state computed at different levels of theory using the CAM-B3LYP/def2-SVP optimized structure.

Level of theory	ΔE_{S1-S0} (eV)	ΔE_{S2-S0} (eV)
CAM-B3LYP/def2-SVP	2.20	2.56
CAM-B3LYP/def2-TZVP	2.19	2.56
ω B97X/def2-SVP	2.21	2.68
ω B97X/def2-TZVP	2.20	2.68
PBE0/def2-SVP	2.18	2.42
PBE0/def2-TZVP	2.17	2.41

3.2 Effect of the level of theory on the fluorescence rate constants

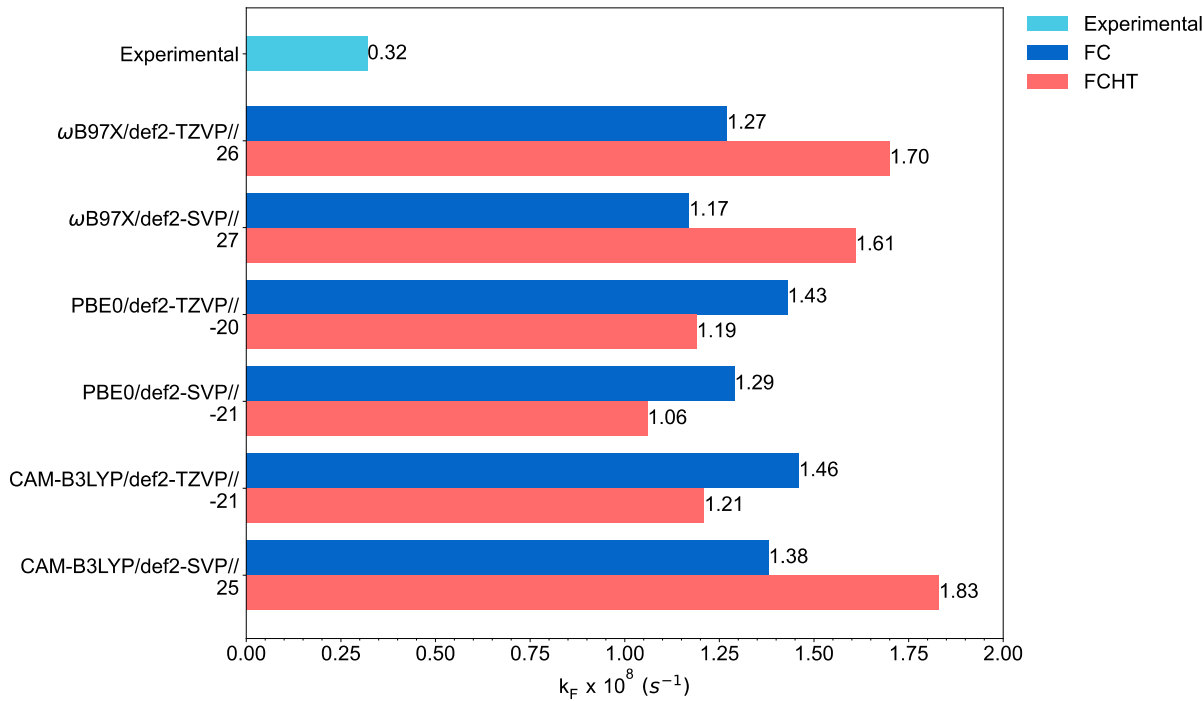


Fig. S12. Fluorescence rate constants calculated at different levels of theory, including Franck-Condon (FC) and Franck-Condon and Herzberg-Teller (FCHT) terms. The CAM-B3LYP/def2-SVP optimized geometry was used in all calculations. The values under the labels are the relative Herzberg-Teller contributions.

3.3 Effect of different parameters on the calculated fluorescence spectra

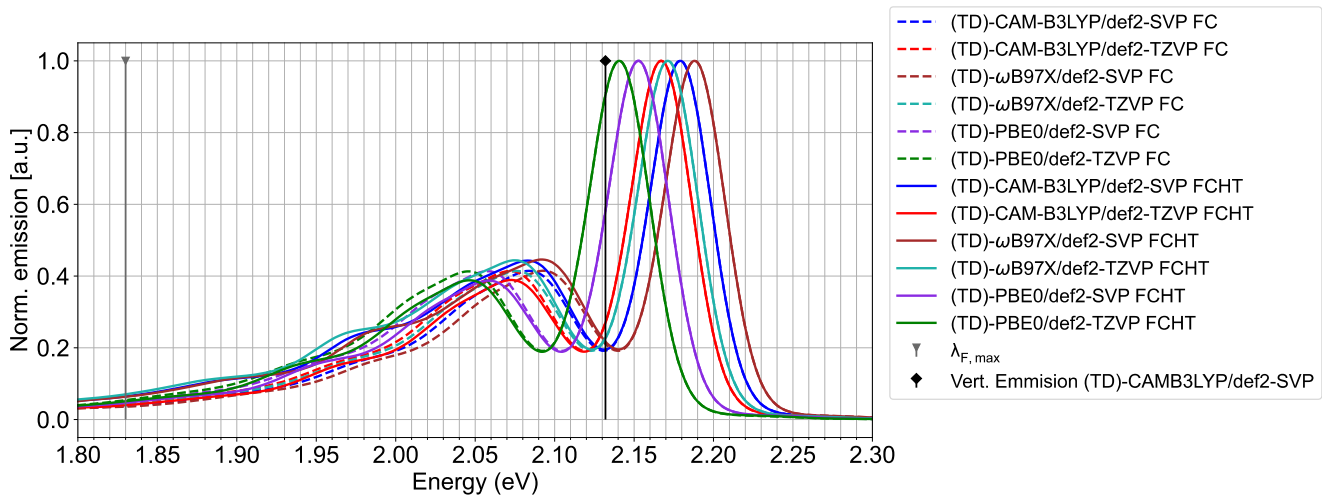


Fig. S13. Predicted fluorescence spectra calculated with different functionals and basis sets including Franck-Condon (FC) and Franck-Condon and Herzberg-Teller (FCHT) terms. The CAM-B3LYP/def2-SVP optimized geometry was used in all calculations. The experimental band maximum is shown in gray.⁴

4. Intersystem crossing

4.1 Adiabatic energy difference between the lowest singlet excited state and the low-lying triplet states

Table S3. Adiabatic energy difference between the lowest singlet excited state and the first, second and third triplet state computed at different levels of theory using the CAM-B3LYP/def2-SVP optimized structure.

Level of theory	ΔE_{S1-T1} (eV)	ΔE_{S1-T2} (eV)	ΔE_{S1-T3} (eV)
CAM-B3LYP/def2-SVP	+0.92	+0.59	+0.13
CAM-B3LYP/def2-TZVP	+0.90	+0.52	+0.11
ω B97X/def2-SVP	+0.94	+0.53	+0.10
ω B97X/def2-TZVP	+0.92	+0.46	+0.07
PBE0/def2-SVP	+0.85	+0.62	+0.16
PBE0/def2-TZVP	+0.84	+0.56	+0.14

4.2 Effect of discarding vibrational modes on the ISC rate constants

Table S4

Spin-orbit coupling matrix elements (SOCMEs, cm⁻¹) and computed ISC rate constants k_{ISC} (s⁻¹) for MPh (298.15K) using the Franck-Condon k_{ISC}^{FC} and Franck-Condon-Herzberg-Teller approximations k_{ISC}^{FCHT} and experimental results at room temperature.

ISC channel	ΔE_{ST} (eV)	$\langle S_1 \hat{H}_{SO} T_i \rangle$	All vibrational modes included		Only vibrational modes above 100 cm ⁻¹ included		k _{ISC} (exp.)
			k _{ISC} ^{FC}	k _{ISC} ^{FCHT}	k _{ISC} ^{FC}	k _{ISC} ^{FCHT}	
S ₁ -T ₁	+0.92	0.16	2.56 x 10 ⁵	1.96 x 10 ⁶	5.80 x 10 ⁵	7.10 x 10 ⁶	7.90 x 10 ⁷ ^a
S ₁ -T ₂	+0.59	0.44	3.19 x 10 ⁶	1.24 x 10 ⁷	3.10 x 10 ⁶	2.08 x 10 ⁷	
S ₁ -T ₃	+0.13	0.10	7.15 x 10 ³	5.61 x 10 ⁴	3.75 x 10 ⁶	3.35 x 10 ⁷	
k _{ISC, total}	-	-	3.45 x 10 ⁶	1.45 x 10 ⁷	7.43 x 10 ⁶	6.14 x 10 ⁷	

^a Ref⁴, toluene (10⁻⁵ M) solution.

4.3 Derivatives of the SOCMEs with respect to the corresponding vibrational modes

Table S5. Harmonic frequencies v_i (cm^{-1}) and triplet-sublevel-averaged ∂SOCMEs (cm^{-1}) with respect to the corresponding vibrational modes at the equilibrium geometry of T_1 , T_2 and T_3 states.

Mode	$v_i@T_1$	$\partial\text{SOCME}_{S_1-T_1}$	Mode	$v_i@T_2$	$\partial\text{SOCME}_{S_1-T_2}$	Mode	$v_i@T_3$	$\partial\text{SOCME}_{S_1-T_3}$
1	100.5	0.000	1	105.4	0.000	1	100.6	0.000
2	108.7	0.000	2	118.5	0.001	2	108.2	0.000
3	118.1	0.000	3	123.2	0.000	3	116.8	0.000
4	122.4	0.000	4	130.6	0.000	4	123.9	0.000
5	126.7	0.000	5	133.4	0.000	5	131.9	0.000
6	132.3	0.000	6	138.3	0.000	6	136.6	0.000
7	135.4	0.000	7	142.0	0.000	7	143.9	0.000
8	141.1	0.000	8	147.4	0.000	8	155.5	0.000
9	144.4	0.000	9	151.5	0.000	9	158.2	0.000
10	157.1	0.000	10	158.3	0.000	10	159.7	0.000
11	164.4	0.000	11	162.8	0.001	11	169.2	0.000
12	173.2	0.000	12	173.1	0.000	12	174.5	0.000
13	186.2	0.000	13	182.0	0.000	13	181.7	0.000
14	189.3	0.000	14	186.3	0.001	14	186.3	0.000
15	195.7	0.000	15	195.5	0.000	15	188.9	0.000
16	196.9	0.000	16	196.3	0.001	16	196.6	0.000
17	211.2	0.000	17	210.4	0.000	17	198.5	0.000
18	213.7	0.000	18	214.8	0.000	18	212.3	0.000
19	223.0	0.000	19	221.1	0.001	19	217.7	0.000
20	233.3	0.000	20	232.8	0.001	20	223.5	0.000
21	239.1	0.000	21	235.9	0.000	21	234.6	0.000
22	246.3	0.000	22	240.3	0.001	22	241.8	0.000
23	252.1	0.000	23	252.9	0.000	23	243.1	0.000
24	257.7	0.000	24	256.3	0.000	24	250.8	0.000
25	263.9	0.001	25	264.5	0.001	25	261.7	0.000
26	267.1	0.000	26	269.6	0.001	26	266.6	0.000
27	272.2	0.000	27	270.4	0.001	27	269.1	0.001
28	276.4	0.000	28	280.0	0.001	28	282.7	0.000

Mode	v_i@T₁	ΔSOCME S₁-T₁	Mode	v_i@T₂	ΔSOCME S₁-T₂	Mode	v_i@T₃	ΔSOCME S₁-T₃
29	286.0	0.000	29	287.0	0.001	29	286.1	0.000
30	291.2	0.000	30	293.9	0.001	30	290.1	0.000
31	296.4	0.000	31	297.9	0.001	31	294.0	0.000
32	316.6	0.000	32	317.3	0.000	32	300.0	0.000
33	321.5	0.001	33	320.5	0.002	33	312.5	0.000
34	345.3	0.000	34	346.1	0.001	34	327.0	0.000
35	362.3	0.000	35	362.9	0.001	35	344.4	0.000
36	368.4	0.000	36	367.4	0.001	36	360.1	0.001
37	383.1	0.002	37	379.1	0.004	37	368.3	0.000
38	386.4	0.001	38	384.0	0.001	38	374.7	0.001
39	409.8	0.000	39	412.7	0.000	39	390.9	0.001
40	429.6	0.001	40	429.6	0.002	40	416.6	0.000
41	443.6	0.001	41	444.4	0.002	41	429.4	0.000
42	462.4	0.001	42	461.5	0.004	42	445.2	0.001
43	469.1	0.002	43	466.2	0.002	43	461.3	0.000
44	480.2	0.001	44	476.6	0.002	44	471.0	0.001
45	493.5	0.002	45	488.9	0.003	45	486.2	0.001
46	521.1	0.003	46	522.3	0.004	46	489.5	0.002
47	538.0	0.003	47	535.3	0.007	47	509.3	0.002
48	552.8	0.002	48	555.1	0.005	48	529.2	0.001
49	575.3	0.000	49	575.7	0.001	49	542.7	0.001
50	593.1	0.000	50	592.2	0.001	50	548.9	0.001
51	610.6	0.001	51	611.3	0.002	51	570.2	0.000
52	615.3	0.000	52	620.5	0.003	52	592.6	0.000
53	620.0	0.001	53	634.2	0.002	53	610.9	0.000
54	639.1	0.001	54	643.7	0.002	54	618.9	0.001
55	650.8	0.002	55	655.5	0.003	55	636.3	0.000
56	663.6	0.001	56	668.9	0.002	56	658.3	0.001
57	673.8	0.001	57	683.6	0.002	57	664.1	0.001
58	685.6	0.001	58	687.3	0.001	58	672.2	0.000
59	691.7	0.000	59	695.3	0.002	59	688.3	0.001
60	706.0	0.000	60	701.6	0.001	60	690.1	0.000

Mode	v_i@T₁	ΔSOCME S₁-T₁	Mode	v_i@T₂	ΔSOCME S₁-T₂	Mode	v_i@T₃	ΔSOCME S₁-T₃
61	707.7	0.000	61	708.3	0.001	61	700.2	0.002
62	720.6	0.001	62	722.8	0.001	62	700.7	0.001
63	721.8	0.000	63	725.9	0.002	63	707.9	0.000
64	725.0	0.001	64	732.4	0.004	64	713.1	0.002
65	730.0	0.002	65	735.8	0.003	65	721.5	0.000
66	732.6	0.000	66	739.3	0.005	66	729.0	0.002
67	753.3	0.001	67	753.9	0.001	67	736.6	0.001
68	755.8	0.001	68	756.0	0.001	68	741.2	0.001
69	768.6	0.001	69	767.9	0.002	69	758.0	0.001
70	776.2	0.000	70	780.2	0.002	70	768.7	0.002
71	782.8	0.000	71	783.6	0.002	71	772.0	0.001
72	789.8	0.002	72	791.5	0.008	72	775.7	0.001
73	795.9	0.002	73	796.6	0.001	73	783.1	0.002
74	799.3	0.001	74	802.3	0.001	74	791.7	0.003
75	801.4	0.003	75	808.4	0.002	75	797.2	0.000
76	812.9	0.001	76	812.8	0.001	76	800.5	0.000
77	833.0	0.001	77	835.5	0.003	77	812.3	0.001
78	846.0	0.001	78	842.3	0.003	78	844.8	0.001
79	853.4	0.001	79	848.1	0.004	79	850.9	0.002
80	869.0	0.001	80	848.2	0.000	80	869.9	0.000
81	876.2	0.000	81	872.0	0.001	81	877.6	0.001
82	891.0	0.002	82	877.7	0.001	82	883.5	0.001
83	902.3	0.000	83	905.1	0.001	83	886.3	0.001
84	908.6	0.000	84	910.6	0.000	84	905.7	0.001
85	916.7	0.000	85	916.6	0.001	85	911.5	0.000
86	931.6	0.000	86	930.5	0.000	86	915.4	0.000
87	940.7	0.000	87	937.6	0.000	87	929.1	0.000
88	948.8	0.000	88	956.9	0.000	88	936.2	0.000
89	956.0	0.000	89	958.3	0.000	89	955.3	0.000
90	963.6	0.001	90	964.2	0.001	90	959.9	0.000
91	989.5	0.000	91	985.5	0.000	91	965.6	0.001
92	994.8	0.001	92	995.7	0.002	92	989.2	0.000

Mode	v_i@T₁	ΔSOCME S₁-T₁	Mode	v_i@T₂	ΔSOCME S₁-T₂	Mode	v_i@T₃	ΔSOCME S₁-T₃
93	996.7	0.000	93	998.8	0.000	93	994.7	0.000
94	1004.6	0.001	94	1016.0	0.000	94	995.2	0.000
95	1014.7	0.000	95	1019.3	0.000	95	1010.6	0.001
96	1025.6	0.001	96	1026.8	0.002	96	1020.6	0.000
97	1038.6	0.000	97	1041.3	0.001	97	1027.7	0.001
98	1041.2	0.000	98	1042.5	0.000	98	1035.1	0.000
99	1045.5	0.001	99	1044.7	0.002	99	1043.0	0.000
100	1047.0	0.001	100	1046.5	0.001	100	1043.5	0.000
101	1057.3	0.001	101	1051.6	0.001	101	1046.6	0.001
102	1071.9	0.000	102	1062.4	0.000	102	1047.3	0.001
103	1078.1	0.001	103	1073.3	0.000	103	1056.6	0.000
104	1087.0	0.001	104	1076.3	0.002	104	1074.6	0.000
105	1090.8	0.000	105	1088.8	0.001	105	1078.4	0.001
106	1096.8	0.001	106	1094.9	0.002	106	1088.6	0.000
107	1104.4	0.001	107	1106.4	0.001	107	1093.5	0.000
108	1126.7	0.000	108	1114.8	0.001	108	1098.4	0.000
109	1133.7	0.000	109	1130.5	0.001	109	1114.7	0.000
110	1136.5	0.001	110	1135.9	0.001	110	1116.4	0.001
111	1138.7	0.001	111	1137.2	0.001	111	1132.2	0.000
112	1144.7	0.000	112	1142.5	0.001	112	1134.3	0.000
113	1152.1	0.000	113	1146.2	0.001	113	1141.9	0.000
114	1157.8	0.000	114	1155.6	0.000	114	1147.0	0.001
115	1174.3	0.001	115	1168.3	0.000	115	1155.6	0.000
116	1177.8	0.000	116	1178.1	0.000	116	1160.6	0.000
117	1178.8	0.000	117	1178.7	0.000	117	1162.3	0.000
118	1187.4	0.000	118	1183.5	0.000	118	1178.5	0.000
119	1199.1	0.000	119	1195.1	0.000	119	1179.2	0.000
120	1203.1	0.000	120	1196.7	0.001	120	1194.2	0.000
121	1211.0	0.000	121	1205.6	0.001	121	1202.7	0.000
122	1212.9	0.001	122	1207.9	0.001	122	1205.6	0.000
123	1223.6	0.001	123	1212.9	0.001	123	1210.9	0.000
124	1227.4	0.000	124	1223.4	0.002	124	1213.4	0.000

Mode	v_i@T₁	ΔSOCME S₁-T₁	Mode	v_i@T₂	ΔSOCME S₁-T₂	Mode	v_i@T₃	ΔSOCME S₁-T₃
125	1234.7	0.001	125	1230.5	0.001	125	1224.5	0.000
126	1241.1	0.001	126	1234.1	0.001	126	1236.6	0.000
127	1244.2	0.000	127	1258.6	0.000	127	1250.5	0.000
128	1265.3	0.000	128	1259.5	0.001	128	1257.3	0.001
129	1272.5	0.000	129	1287.5	0.000	129	1264.1	0.000
130	1287.9	0.000	130	1288.3	0.000	130	1279.8	0.000
131	1289.4	0.000	131	1292.8	0.001	131	1288.8	0.000
132	1306.8	0.001	132	1305.3	0.001	132	1293.9	0.000
133	1310.4	0.001	133	1307.9	0.001	133	1303.3	0.001
134	1311.5	0.000	134	1323.7	0.001	134	1307.5	0.000
135	1325.5	0.000	135	1326.8	0.000	135	1318.0	0.001
136	1331.3	0.000	136	1341.8	0.001	136	1323.4	0.001
137	1343.1	0.000	137	1358.6	0.001	137	1325.1	0.001
138	1346.8	0.001	138	1365.4	0.002	138	1331.0	0.000
139	1362.2	0.001	139	1371.6	0.000	139	1345.1	0.000
140	1372.6	0.001	140	1377.2	0.000	140	1368.3	0.000
141	1379.0	0.000	141	1379.2	0.001	141	1372.8	0.001
142	1383.6	0.000	142	1389.6	0.000	142	1378.3	0.000
143	1389.6	0.001	143	1397.2	0.001	143	1385.9	0.000
144	1394.1	0.000	144	1398.2	0.000	144	1390.5	0.000
145	1396.3	0.001	145	1401.8	0.000	145	1393.8	0.000
146	1398.4	0.000	146	1406.9	0.000	146	1397.8	0.000
147	1400.6	0.000	147	1413.9	0.000	147	1398.3	0.000
148	1413.4	0.000	148	1418.1	0.000	148	1407.1	0.001
149	1417.6	0.000	149	1427.1	0.001	149	1411.8	0.000
150	1423.1	0.000	150	1431.8	0.000	150	1416.7	0.000
151	1435.7	0.000	151	1440.2	0.000	151	1424.2	0.000
152	1442.3	0.000	152	1446.1	0.000	152	1430.7	0.001
153	1447.3	0.000	153	1447.6	0.000	153	1443.2	0.000
154	1449.7	0.000	154	1450.1	0.001	154	1446.3	0.000
155	1450.2	0.000	155	1452.2	0.000	155	1448.6	0.000
156	1451.6	0.000	156	1455.5	0.000	156	1454.2	0.000

Mode	v_i@T₁	ΔSOCME S₁-T₁	Mode	v_i@T₂	ΔSOCME S₁-T₂	Mode	v_i@T₃	ΔSOCME S₁-T₃
157	1454.2	0.000	157	1455.5	0.001	157	1454.9	0.000
158	1456.2	0.000	158	1458.4	0.000	158	1455.9	0.000
159	1456.9	0.000	159	1458.8	0.000	159	1456.9	0.000
160	1457.9	0.000	160	1459.3	0.000	160	1458.6	0.000
161	1458.1	0.000	161	1462.4	0.000	161	1459.4	0.000
162	1463.0	0.001	162	1463.8	0.000	162	1461.3	0.000
163	1464.1	0.000	163	1464.7	0.000	163	1461.5	0.000
164	1464.4	0.001	164	1465.5	0.000	164	1462.7	0.000
165	1464.8	0.000	165	1466.0	0.000	165	1464.0	0.000
166	1465.7	0.000	166	1466.2	0.000	166	1464.3	0.000
167	1466.1	0.000	167	1466.4	0.000	167	1464.7	0.000
168	1466.3	0.000	168	1467.4	0.000	168	1466.2	0.000
169	1467.4	0.000	169	1470.2	0.000	169	1467.1	0.000
170	1478.0	0.000	170	1473.9	0.000	170	1473.1	0.000
171	1482.8	0.000	171	1478.4	0.000	171	1474.6	0.001
172	1484.1	0.000	172	1483.5	0.000	172	1477.9	0.000
173	1486.3	0.001	173	1484.3	0.000	173	1479.3	0.001
174	1490.4	0.001	174	1488.4	0.000	174	1483.9	0.000
175	1517.9	0.001	175	1532.9	0.000	175	1487.5	0.000
176	1538.0	0.001	176	1551.2	0.001	176	1500.7	0.001
177	1547.4	0.001	177	1559.2	0.000	177	1507.8	0.000
178	1556.8	0.000	178	1600.6	0.000	178	1532.6	0.000
179	1576.1	0.001	179	1620.6	0.000	179	1589.5	0.000
180	1600.0	0.001	180	1629.2	0.001	180	1622.8	0.000
181	1632.3	0.001	181	1661.5	0.000	181	1634.2	0.001
182	1642.4	0.002	182	1705.8	0.000	182	1644.7	0.000
183	1677.3	0.002	183	1720.4	0.000	183	1663.1	0.000
184	1720.7	0.000	184	1732.6	0.000	184	1667.9	0.000
185	1730.1	0.000	185	1818.2	0.000	185	1723.5	0.000
186	1733.0	0.001	186	1844.3	0.000	186	1842.0	0.000
187	1831.0	0.000	187	1848.9	0.001	187	1843.9	0.000
188	1842.7	0.000	188	2115.5	0.001	188	1858.1	0.000

Mode	v_i@T₁	ΔSOCME S₁-T₁	Mode	v_i@T₂	ΔSOCME S₁-T₂	Mode	v_i@T₃	ΔSOCME S₁-T₃
189	1851.9	0.000	189	2971.5	0.001	189	1951.0	0.002
190	3052.1	0.000	190	3051.3	0.000	190	2722.8	0.022
191	3052.1	0.000	191	3052.1	0.000	191	3042.8	0.000
192	3052.7	0.000	192	3052.5	0.000	192	3050.1	0.000
193	3054.1	0.000	193	3054.6	0.000	193	3054.3	0.000
194	3054.6	0.000	194	3055.0	0.000	194	3054.9	0.000
195	3065.8	0.000	195	3066.6	0.000	195	3056.2	0.000
196	3068.8	0.000	196	3072.1	0.000	196	3062.2	0.000
197	3071.6	0.000	197	3072.5	0.000	197	3066.1	0.001
198	3072.1	0.000	198	3075.8	0.001	198	3072.5	0.000
199	3077.6	0.000	199	3078.3	0.000	199	3073.2	0.000
200	3084.9	0.000	200	3086.5	0.000	200	3077.9	0.000
201	3093.1	0.000	201	3094.4	0.001	201	3084.4	0.000
202	3094.2	0.000	202	3096.9	0.001	202	3089.3	0.000
203	3115.0	0.000	203	3111.9	0.000	203	3091.4	0.000
204	3125.5	0.000	204	3120.3	0.000	204	3107.6	0.000
205	3125.6	0.000	205	3121.7	0.000	205	3108.9	0.000
206	3128.7	0.000	206	3128.2	0.000	206	3128.8	0.000
207	3132.8	0.000	207	3135.1	0.000	207	3133.9	0.000
208	3145.6	0.000	208	3141.3	0.000	208	3134.1	0.000
209	3145.9	0.000	209	3142.5	0.000	209	3140.4	0.000
210	3148.2	0.000	210	3146.2	0.000	210	3144.1	0.000
211	3150.0	0.000	211	3149.2	0.000	211	3145.2	0.000
212	3151.4	0.000	212	3149.7	0.000	212	3151.3	0.000
213	3161.3	0.000	213	3156.9	0.000	213	3152.2	0.000
214	3164.4	0.000	214	3160.0	0.000	214	3152.3	0.000
215	3165.5	0.000	215	3164.8	0.000	215	3165.2	0.000
216	3167.0	0.000	216	3166.6	0.000	216	3166.4	0.000
217	3170.4	0.000	217	3170.4	0.000	217	3168.1	0.000
218	3175.0	0.000	218	3171.5	0.000	218	3170.8	0.000
219	3188.4	0.000	219	3181.5	0.000	219	3175.7	0.000
220	3201.4	0.000	220	3201.5	0.000	220	3183.2	0.000

Mode	$v_i@T_1$	$\partial SOCME_{S_1-T_1}$	Mode	$v_i@T_2$	$\partial SOCME_{S_1-T_2}$	Mode	$v_i@T_3$	$\partial SOCME_{S_1-T_3}$
221	3203.2	0.000	221	3202.2	0.000	221	3201.9	0.000
222	3229.0	0.000	222	3231.2	0.000	222	3204.0	0.000
223	3235.2	0.000	223	3246.8	0.000	223	3227.7	0.001
224	3237.4	0.000	224	3248.2	0.000	224	3229.5	0.000
225	3281.9	0.000	225	3271.6	0.000	225	3239.9	0.001
226	3529.6	0.000	226	3431.2	0.000	226	3276.6	0.000
227	3635.4	0.000	227	3596.2	0.000	227	3515.7	0.001
-	-	-	-	-	-	228	3652.6	0.002

4.4 Effect of the Gaussian linewidth on the ISC rate constants

Table S6. Effect of the Gaussian linewidth on the ISC rate constants k_{ISC} at room temperature.

Channel	Parameters		k_{ISC}^{FCHT} (s ⁻¹)
	ΔE_{ST} (eV)	Gaussian linewidth η (cm ⁻¹)	
$S_1 \rightsquigarrow T_1$	+0.92	0.1	7.10×10^6
$S_1 \rightsquigarrow T_1$	+0.92	1.0	7.10×10^6
$S_1 \rightsquigarrow T_1$	+0.92	10.0	7.10×10^6
$S_1 \rightsquigarrow T_1$	+0.92	100.0	7.11×10^6
$S_1 \rightsquigarrow T_2$	+0.59	0.1	2.08×10^7
$S_1 \rightsquigarrow T_2$	+0.59	1.0	2.08×10^7
$S_1 \rightsquigarrow T_2$	+0.59	10.0	2.08×10^7
$S_1 \rightsquigarrow T_2$	+0.59	100.0	2.11×10^7
$S_1 \rightsquigarrow T_3$	+0.13	0.1	3.32×10^7
$S_1 \rightsquigarrow T_3$	+0.13	1.0	3.34×10^7
$S_1 \rightsquigarrow T_3$	+0.13	10.0	3.35×10^7
$S_1 \rightsquigarrow T_3$	+0.13	100.0	3.39×10^7

4.5 Effect of the level of theory, FC and FCHT approximations on the k_{ISC}

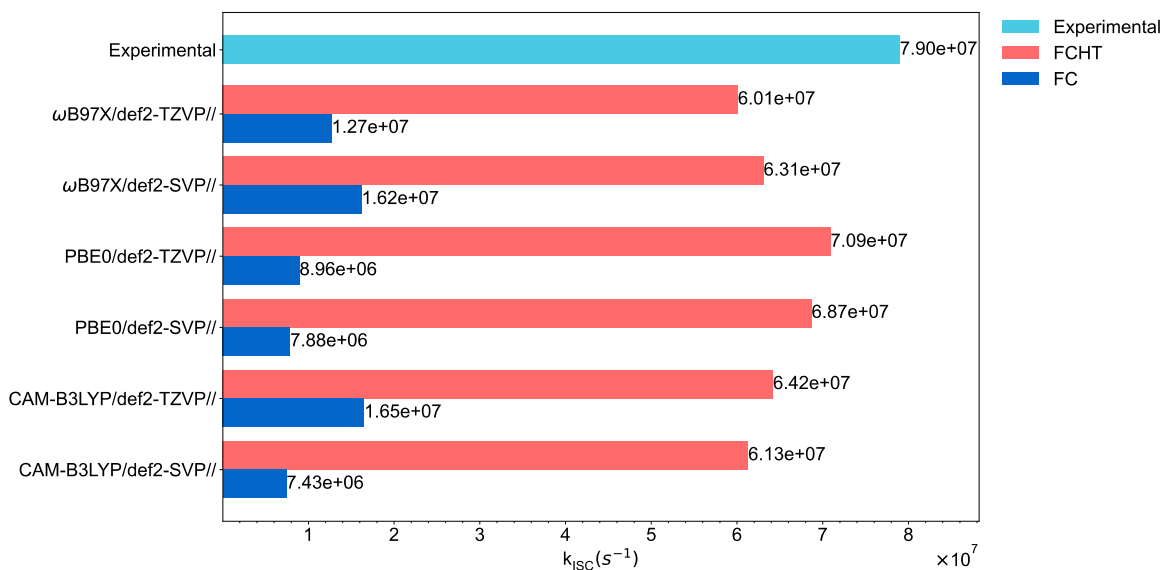
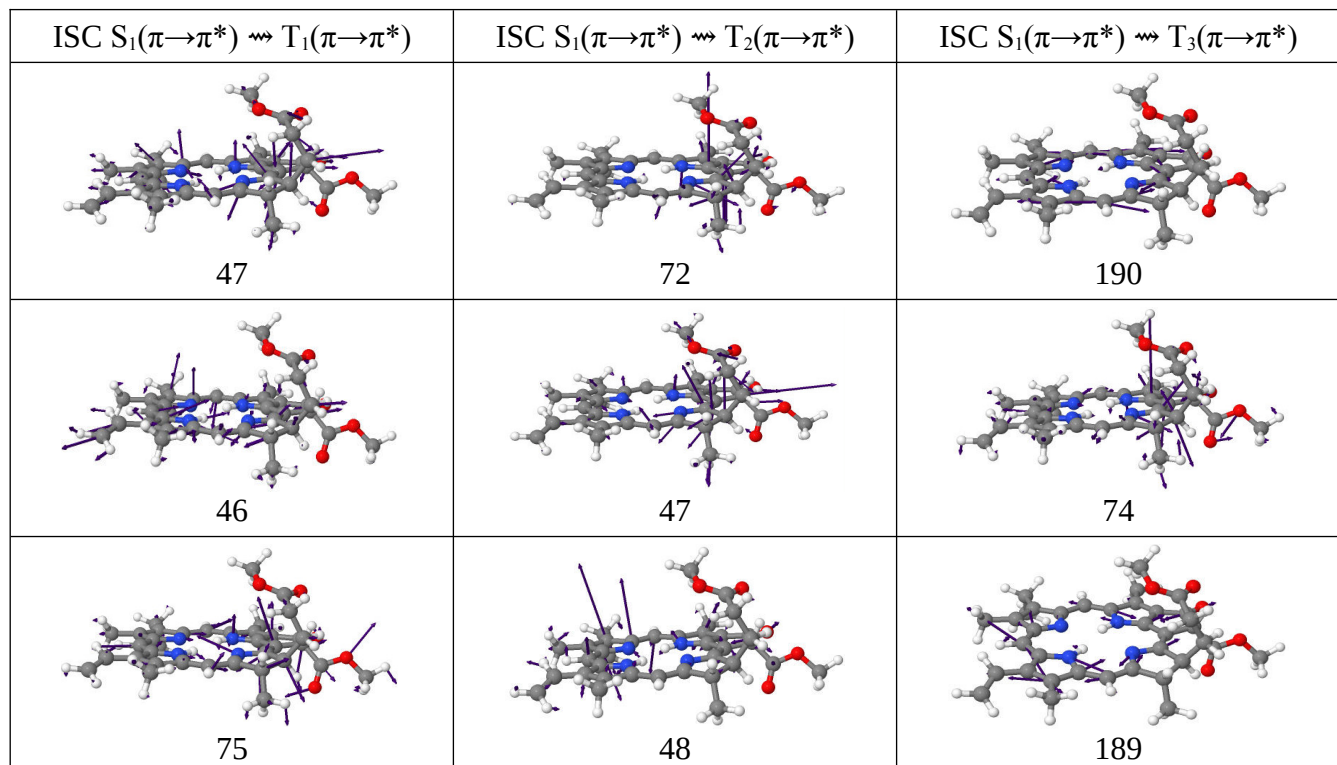


Fig. S14. Effect of the level of theory on the ISC rate constants k_{ISC} employing the FC (Franck-Condon) and Franck-Condon-Herzberg-Teller (FCHT) approximations. All calculations were performed at the CAM-B3LYP/def2-SVP optimized geometries, and using the SOCMEs calculated at the CAM-B3LYP/def2-SVP level of theory.

4.6 The five largest coupling vibrational normal modes



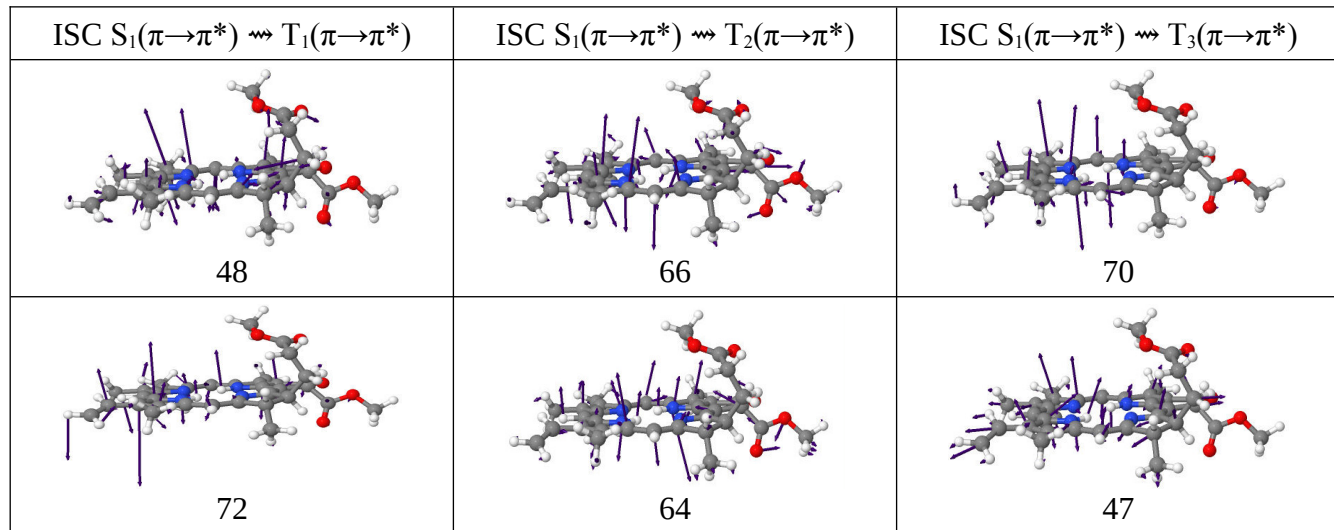


Fig. S15. The five largest coupling vibrational normal modes calculated at their own $T_n(\pi \rightarrow \pi^*)$ minimum of methylpheophorbide a (MPhe).

References

- 1 A. G. Martynov, J. Mack, A. K. May, T. Nyokong, Y. G. Gorbunova and A. Y. Tsivadze, Methodological Survey of Simplified TD-DFT Methods for Fast and Accurate Interpretation of UV–Vis–NIR Spectra of Phthalocyanines, *ACS Omega*, 2019, **4**, 7265–7284.
- 2 S. Bai, R. Mansour, L. Stojanović, J. M. Toldo and M. Barbatti, On the origin of the shift between vertical excitation and band maximum in molecular photoabsorption, *J. Mol. Model.*, 2020, **26**, 107.
- 3 I. Balashova, A. Tolbin, P. Tarakanov, A. Krot, K. Fedorova, I. Sergeeva, S. Trashin, K. De Wael, V. Pushkarev, M. Koifman and G. Ponomarev, A Covalently Linked Dyad Based on Zinc Phthalocyanine and Methylpheophorbide a: Synthetic and Physicochemical Study, *MACROHETEROCYCLES*, 2021, **14**, 40–50.
- 4 K.-K. Wang, J. Li, B.-J. Kim, J.-H. Lee, H.-W. Shin, S.-H. Ko, W.-Y. Lee, C.-H. Lee, S. H. Jung and Y.-R. Kim, Photophysical Properties of Pheophorbide-a Derivatives and Their Photodynamic Therapeutic Effects on a Tumor Cell Line *In Vitro*, *Int. J. Photoenergy*, 2014, **2014**, 793723, 1–7.